Comparison of Leader and Tail Switching with Full Shuffle in Swarming V-shaped drones: Efficiency and Sensitivity Analysis

Amir Mirzaeinia[1], Mehdi Mirzaeinia[2], Mostafa Hassanalian[3]*

V-shaped formation helps drones to consume less energy for flight. It is shown that different drag loads will be applied to various drones in a V-shaped swarm. The sensitivity of the drag of each drone to the wingspan and wingtip spacing in a V-shaped swarm is investigated. A load-balancing mechanism through lead-and-tail replacement is carried out in swarming drones and the flying distance improvement is analyzed. Moreover, in this paper, two different shuffling scenarios are compared with the head-and-tail replacement mechanisms. In the first shuffling method, the maximum-energy drone is replaced with the minimum-energy drone, iteratively. In the second shuffling method, the first two maximum-energy drones are repositioned with the leader and the tail drone, and the second two maximum go to the drone after the first and before the last drone. A similar process is applied for the rest of the drones. It is found that an optimum replacement mechanism can be defined for swarming drones in order to enhance their flight efficiency.

I. Introduction

For a decade, drones have received more attention than before, which has led to the development of a wide range of them with various shapes[1-5]. Recent autonomous aerial vehicles are classified in a broad spectrum and equipped with sophisticated sensors[6]. These drones are able to operate in urban environments as well as confined spaces depending on their sizes and configurations[7-10]. There are different methods to improve the energy efficiency of drones, such as optimization in the design process[11-13]. However, swarming and formation flight can be considered as one of the effective approaches for drag reduction[14]. V-shaped flight formation has been studied for more than fifty years[11]. Different aspects of flight formation, such as aerodynamics, control, and energy conservation have been investigated on migrating birds and drones[15-17].

In 1974, Heppner presented a different classification for flight formation of birds and discussed the possible advantages of each formation[18]. In 1981, Badgerow and Hainsworth analyzed the saving energy through V-shaped formation flight. They studied different spacing and consequent saving energy on the flocking of migrating birds[19]. Hummel in 1982 proposed theoretical aerodynamic modeling to calculate the flight power reduction for arbitrarily shaped flight formations with any number of birds. He showed that the total reduction in-flight power of the whole formation strongly depends on the lateral distance of the wingtips of the birds and a longitudinal displacement in flight direction has no influence[20].

In 2002, Seiler et al. studied the two aspects of migrating birds V-shaped formations including their aerodynamics advantages and improvement of their visual communication. They applied a systems theory approach to show that the birds need to keep their formations small. They demonstrated that if the formations become large, then the birds at the end of formations would have difficulty keeping their positions in the formation[21]. Andersson and Wallander in 2003 explored different types of flight formation of migrating birds, including V-shaped and echelon flocking flights. They suggested that kin selection plays an important role in flight formations of flocking birds and the leading position in V formation is more expensive energetically than are other positions[22].

In 2007, Thien et al. investigated the V-shaped swarming flight of birds and generated vortices including downwash and upwash effects. Drag reduction of the leader and follower birds were also analyzed in their study[23]. In 2008, Nathan and Barbosa considered flocks of artificial birds and studied the emergence of V-shaped formations during flight. In their study, they introduced a set of fully distributed posi-

[1] PhD. student, Department of Computer Science and Engineering, New Mexico Tech, Socorro, NM 87801, USA.

[2] Ms. Student, Department of Electrical Engineering, AmirKabir University of Technology, Tehran, Iran.

[3] Assistant Professor, Department of Mechanical Engineering, New Mexico Tech, Socorro, NM 87801, USA (*Corresponding).

tioning rules to guide the birds' movements and demonstrated that artificial birds tend to lead to stabilization into several of the well-known V-shaped formations[24]. In 2009, Bajec and Heppner reviewed different aspects of the V-shaped formation in birds[25].

Commercial formation flight has been studied by many researchers for a long time[26-30]. It has been shown that this formation flight can dramatically reduce the required energy without fundamental changes to the aircraft flying[26-30]. As an example, Bower et al. in 2009, investigated the use of formation flight on five FedEx flights from the pacific northwest to Memphis, TN[26]. Quantifying the achievable fuel burn reduction in a commercial setting without changing the flight schedule was the main objective of their study. They showed that a fuel saving of 4 % can be achieved if the distance between the wingtips of airplanes is 10 % of their wingspan. It was demonstrated that the fuel consumption can be decreased by up to 11.5 % if the tip-to-tip overlap of about 10% of the wingspan[26].

In 2011, Ning et al. examined more practical techniques to formation flight called extended formation flight, which benefits of the durability of cruise wakes and extends the streamwise spacing between the aircraft by at least ten spans[27]. They found for spacing around 10 to 40 spans, two aircraft formation has a maximum induced drag reduction of 30±3% and this reduction for three aircraft is 40±6%[27]. In 2012, Pahle and Berger investigated the formation flight for drag reduction on the C-17 aircraft[28]. They analyzed the flight data collected during several two-ship, C-17 formation flights at a single flight condition[28]. Kent and Richards in 2013 explored an extension to a geometric approach of finding optimal routes for commercial formation flight of aircraft in order to decrease overall fuel burn[29]. Kless et al. in 2013 conducted an analysis of extended formations of the flying airplanes[23]. They found that in an extended formation of flying airplanes, with a separation distance of tens of wingspan a significant fuel saving can be achieved. Their analysis showed that more than 90 % of energy benefits can be obtained with a 10% variation in spanwise and 5% variation in vertical positions[30].

In 2017, Li et al. studied how to form a V-shaped formation observed in migrating birds from a control engineering perspective. Besides considerations of collision avoidance and energy consumptions, the biological perception model in terms of the visual communication constraints was also investigated by them[31]. They showed that by incorporating the visual communication constraints into the cost function, a standard gradient-based control algorithm can form the formation flight. Colombi et al. in 2017 modified the proposed approach by Reynolds and presented an algorithm for unmanned aerial vehicles in a swarming flight which maintains a precise position relative to the preceding UAV. In their study, they showed that UAVs in a V-shaped formation experiences a decrease in their induced drag that consequently results in the reduction of their overall fuel consumption and enhancement in their flight range and endurance[14].

In "V" formation flight, the leading drone generates air disturbance that helps the follower drones to consume less energy for flight. In "V" formation flight, the wings of each fixed-wing drone produce vortices due to the pressure difference of the top and bottom sides of the wings. This wake turbulence vortex generates an upwash outboard of the wingtips and a downwash inboard of the wingtips. Wingtip spacing is one of the key factors which is affecting the total and individual drag force of each drone. This is investigated over the previous research studies. Other studies show that the fixed-wing drones in the middle and tail have to deal with more drag force than the others in the middle. This imbalance load distribution leads to more recent studies to apply load balancing through V-shaped reformation. Mirzaeinia et. al in[11] investigate the effect of replacing the lead and tail with middle flights. Their studies revealed that the replacement scenario helps to balance the drag load during the flight. In this study, the comparison of leader and tail switching with full shuffle in swarming V-shaped drones is carried out.

I. Drag of Individual and Swarming Drones

It should be noted that in this study, analytical fluid dynamics is carried out with corresponding assumptions to model the aerodynamics of the V-shaped formation flight. In the following drag modeling, it is assumed that fixed-wing drones are flying in a laminar regime of flow (low Reynolds number). The type of flow is assumed to be incompressible; therefore, the air density is considered constant during the analysis. Since the drones are generally using the electric motors and batteries for their propulsion, the density of the air is not affected too much compared to the higher speed manned aircraft. In swarming, each drone generates downwash and upwash effects. It is assumed that the downward velocity (downwash) created by the wing of the drone is constant along the span and lack of the turbulence within the wake[11].

In this modeling, it is assumed that the total induced drag of the swarming fixed-wing drones depends on the scatter along the y-axis and not on the depth distribution along the x-axis. The total drag of swarming drones is calculated as bellows[11]:

$$D_I(n) = n \times D_{I11} + \frac{4D_{I11}}{\pi^2} \sum_{i=1}^{n-1} \sum_{j=i+1}^{n} loglog\left[1 - \left(\frac{2a}{\left|i-j\right|(b+s)}\right)^2\right] \tag{1}$$

where n is the number of drones, D_{I11}, b, a, and s are the induced drag of a fixed-wing drone, wingspan, the half of the length of the bound vortex, and distance between adjacent drones perpendicular to the flight path, respectively. The total drag of each drone considering is calculated by[11]:

$$D_{Ik} = D_{I11} + \frac{2D_{I11}}{\pi^2} loglog \prod_{j=1}^{n} \left[1 - \left(\frac{2a}{\left|k-j\right|(b+s)}\right)^2\right] \tag{2}$$

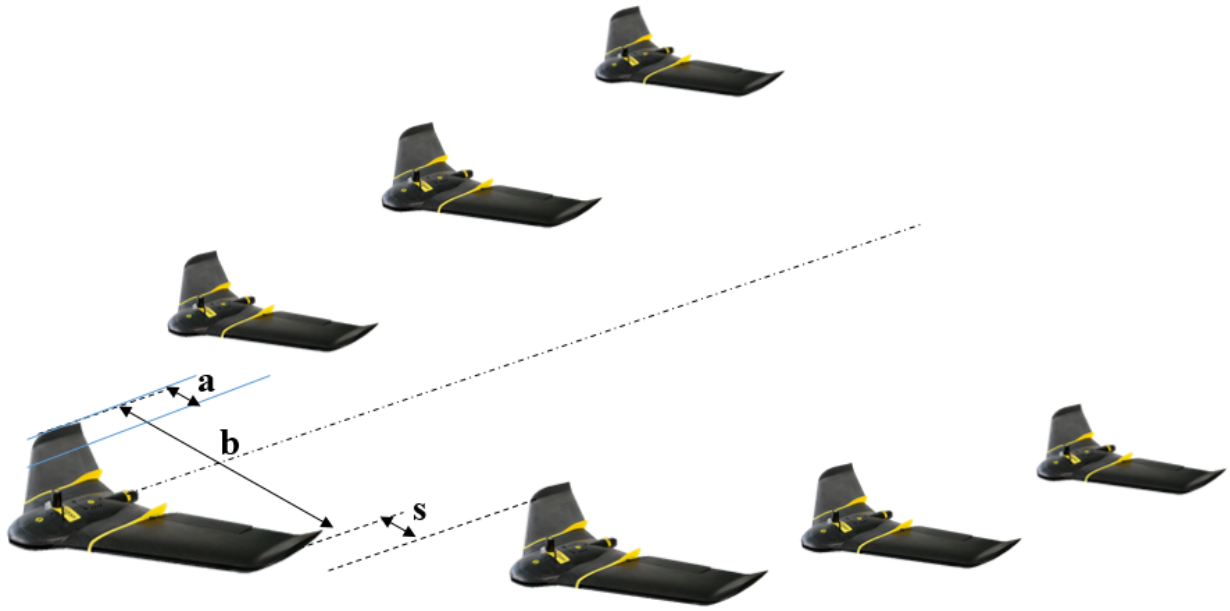

Figure 1. View of the swarming fixed-wing drones with V-shaped formation.

In this study, EBee Sensfly Flying Wing is considered for a possible swarming flight as a commercialized drone. The characteristics of the selected fixed-wing drone are shown in Table 1.

Table 1. The specifications of the EBee Sensfly Flying Wing[32].

Specification	Value
Wingspan (m)	1.1
Flying Weight (kg)	1.1
Maximum Flying Time (Minutes)	59
Cruise Speed (m/s)	11-30 (15)

III. Sensitivity Analysis of Swarm Parameters

In this work, sensitivity analysis is carried out to study the effects of each swarm parameter. The sensitivity of the ratio of induced drag and individual drag of swarming drones to the independent parameters, such as wingspan (b) and wingtip spacing (s) is investigated. The reference values for b and s are equal to 1.1 m and 0.055 m, respectively. Sensitivities of ±5%, ±10%, ±15% are considered in this analysis. In Table 2, the values of each parameter are shown.

Table 2. Values of swarm parameters.

Parameter	Wingspan (b, m)	Wingtip spacing (s, m)
Wingspan	0.935, 0.99, 1.045, 1.1, 1.155, 1.21, 1.265	0.055
Wingtip spacing	1.1	0.04675, 0.0495, 0.05225, 0.055, 0.05775, 0.0605, 0.06325

In Figures 2(a) and 2(b), the sensitivities of the ratio of induced drag (formation/solo flight) to the wingtip spacing and wingspan are shown, respectively. The results in Figure 2(a) indicate that with increasing the wingtip spacing from the reference value, the ratio of induced drag is increased. Figure 2(b) demonstrates that with increasing the wingspan of the drones from the reference value, the ratio of induced drag is decreased. Figures 2(a) and 2(b) also show the sensitivity of the ratio of the induced drag to the number of the drones[11].

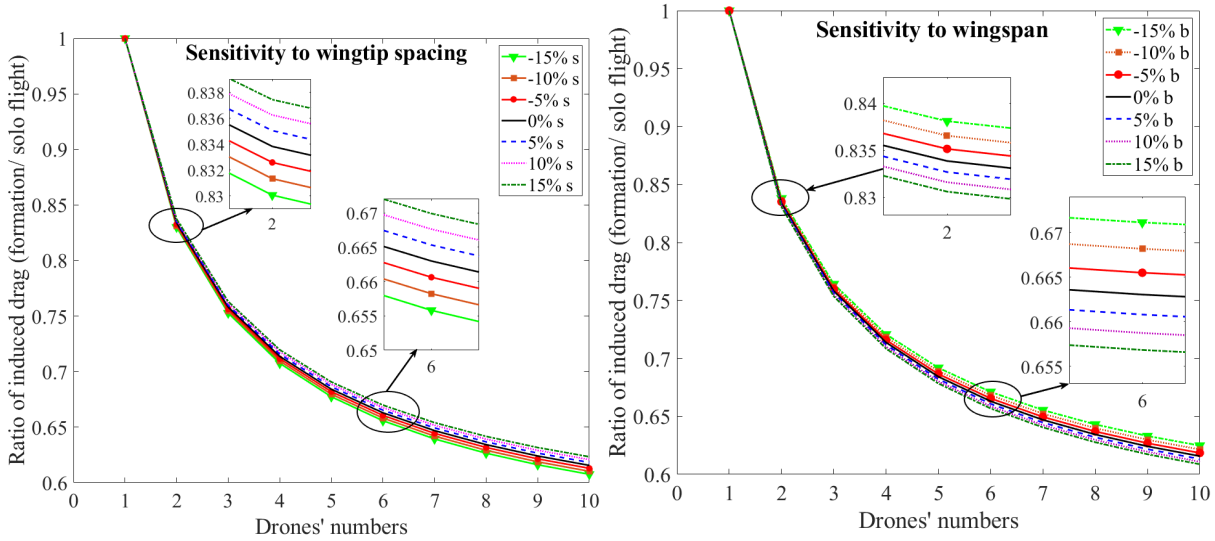

(a) **(b)**

Figure 2. The sensitivity of the ratio of induced drag to the (a) wingtip spacing and (b) wingspan.

In Table 3, for different numbers of the drones in a swarm, the sensitivity of the ratio of induced drag (formation/solo flight) to the wingtip spacing and wingspan is shown. As it is apparent from Table 3, a deviation of ±5 % in wingtip spacing and wingspan results in an almost similar reduction or increment in the formation/solo flight induced drag. It should be noted that in Table 3, the values have been calculated compared to the reference values (0% s or b). For the deviations of the -10% and -15%, the magnitudes of the percentages due to the changes in wingspan are more than the changes in wingtip spacing. For the deviations of 10% and 15%, the magnitudes of the percentages in the formation/solo flight induced drag are higher for wingtips spacing compared to the wingspan. It also can be seen that with increasing the number of drones in swarm, the magnitudes of the percentages are increasing[11].

Table 3. The sensitivity of the formation/solo flight induced drag to the wingtip spacing and wingspan.

Number of drones	**2**	**3**	**4**	**5**	**6**	**7**	**8**	**9**	**10**

Sensitivity (%)	2	3	4	5	6	7	8	9	10
-15% *s*	-0.44	-0.70	-0.87	-0.99	-1.09	-1.16	-1.21	-1.27	-1.30
-15% *b*	0.50	0.79	0.98	1.11	1.22	1.30	1.37	1.43	1.48
-10% *s*	-0.30	-0.46	-0.57	-0.66	-0.72	-0.76	-0.80	-0.83	-0.86
-10 % *b*	0.31	0.50	0.62	0.70	0.77	0.83	0.87	0.90	0.94
-5% *s*	-0.14	-0.24	-0.28	-0.32	-0.36	-0.37	-0.39	-0.42	-0.42
-5 % *b*	0.14	0.24	0.29	0.34	0.36	0.40	0.41	0.43	0.45
5% *s*	0.14	0.22	0.28	0.32	0.35	0.39	0.39	0.42	0.44
5 % *b*	-0.14	-0.21	-0.28	-0.32	-0.34	-0.36	-0.38	-0.40	-0.41
10% *s*	0.29	0.45	0.56	0.64	0.69	0.76	0.79	0.82	0.84
10 % *b*	-0.28	-0.42	-0.53	-0.60	-0.66	-0.70	-0.74	-0.77	-0.78
15% *s*	0.43	0.67	0.84	0.95	1.04	1.11	1.17	1.22	1.27
15 % *b*	-0.40	-0.60	-0.76	-0.86	-0.95	-1.00	-1.06	-1.11	-1.14

The sensitivities of the drag of each drone in a swarm with 10 drones to the wingtip spacing and wingspan, are shown in Figures 3(a) and 3(b), respectively. It can be seen that the drag of each drone in swarm increases with increasing the wingtip spacing and decreasing the wingspan.

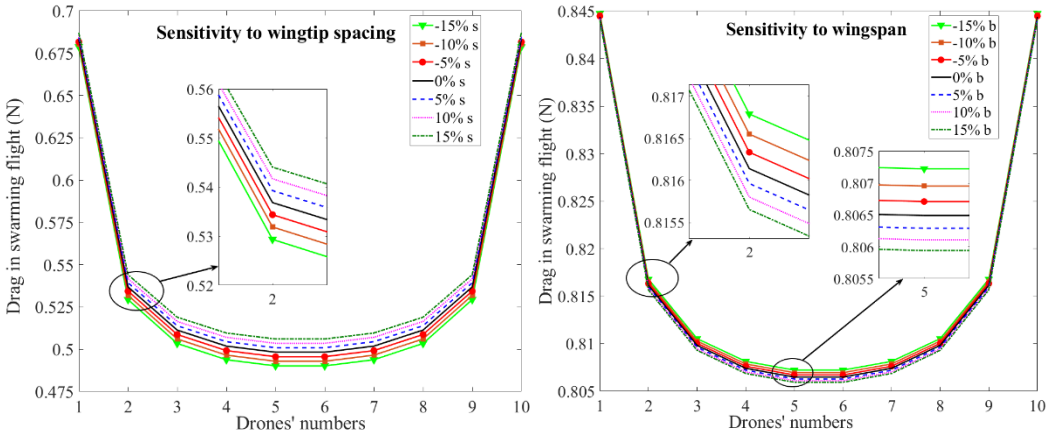

(a) **(b)**

Figure 3. The sensitivity of the drag of each drone in the swarm to the (a) wingtip spacing and (b) wingspan.

In Table 4, for 10 drones in a swarm, the sensitivity of the drag of each drone to the wingtip spacing and wingspan is shown. As shown in Table 4, increasing the wingspan and decreasing the wingtip spacing reduces the drag of each drone in the swarm.

Table 4. The sensitivity of the drag of each drone in swarm to the wingtip spacing and wingspan.

Drones' numbers	1	2	3	4	5

Sensitivity (%)	1	2	3	4	5
-15% *s*	-0.60	-1.40	-1.54	-1.59	-1.63
-15% *b*	0.69	1.60	1.74	1.81	1.85
-10% *s*	-0.40	-0.91	-1.02	-1.06	-1.08
-10 % *b*	0.44	1.00	1.11	1.16	1.18
-5% *s*	-0.19	-0.45	-0.51	-0.52	-0.54
-5 % *b*	0.20	0.48	0.53	0.56	0.56
5% *s*	-0.20	0.47	0.51	0.54	0.52
5 % *b*	-0.19	-0.42	-0.49	-0.50	-0.50
10% *s*	0.41	0.91	1.00	1.04	1.04
10 % *b*	-0.37	-0.84	-0.92	-0.96	-0.96
15% *s*	0.60	1.36	1.49	1.55	1.57
15 % *b*	-0.54	-1.21	-1.33	-1.37	-1.40

IV. Algorithms for Individual Drag Calculation and Replacement Mechanisms in Swarm

The following algorithms are applied to demonstrate the replacement mechanisms and load balancing. The first algorithm shows the leader and tail switching in the swarm, and the second and third algorithms indicate the two different approaches for a full shuffle in swarming V-shaped drones, respectively.

Algorithm 1: Replacement mechanism with leader and tail switching

```
1:  Function Leader_and_tail_Swapping (a, s , b , N , v , init_energy)
    d_11 = (2 * m^2 * 9.8 ^ 2) / (pi * 1.225 * b ^ 2 * v ^ 2); % induced drag of one drone
2:  D_total = Drag_Calculation_function (a,s,b,N,d_11); % Vector contains drag of all drones
3:  While (min ( Remind energy) > 0.01 * initial energy)
4:      Distance = 0.5 * Remind Energy of the leader/ D_total (1)
5:      Remind Energy=  Remind Energy  - Distance * D_total      % Vector contains remind energy of  all
    drones
6:      Swap(leader, drone with maximum energy)
7:      Swap(tail, drone with second maximum max energy)
8:  End Function
```

Algorithm 2: Replacement mechanism for full shuffle (1)

```
1:  Function Shuffle (a, s, b, N, v, init_energy)
    d_11 = (2 * m^2 * 9.8 ^ 2) / (pi * 1.225 * b ^ 2 * v ^ 2); % induced drag of one drone
2:  D_total = Drag_Calculation_function (a,s,b,N,d_11); % Vector contains drag of all drones
3:  While (min ( Remind energy) > 0.01 * initial energy)
4:      Distance = 0.5 * Remind Energy of the leader/ D_total (1)
5:      Remind Energy= Remind Energy - Distance * D_total % Vector contains remind energy of all
    drones
6:      for i=1:floor(length(b)/2)
7:          max_ind = find(maximum remained energy);
8:          min_ind = find(minimum remained energy);
9:          Swam (max_ind, min_ind)
10:     End
11: End Function
```

Algorithm 3: Replacement mechanism for full shuffle (2)

```
1:  Function Shuffle (a, s, b, N, v, init_energy)
    d_11 = (2 * m^2 * 9.8 ^ 2) / (pi * 1.225 * b ^ 2 * v ^ 2); % induced drag of one drone
2:  D_total = Drag_Calculation_function (a,s,b,N,d_11); % Vector contains drag of all drones
3:  While (min ( Remind energy) > 0.01 * initial energy)
4:      Distance = 0.5 * Remind Energy of the leader/ D_total (1)
5:      Remind Energy= Remind Energy - Distance * D_total % Vector contains remind energy of all
    drones
6:      Sorted_energy = Sort(remained energy, Descending)
7:      for i=1:floor(length(b)/2)
8:          Swap (remained energy (i), Sorted_energy. next) %swap the max with the leaders
9:          Swap (remained energy(end-i), Sorted_energy. next) % swap the max with the followers
10:     End
11: End Function
```

V. Comparison of Leader and Tail Switching with Two Types of Full Shuffle

The wingtip spacing (*s*) between drones is considered as:

$$s = 0.5b(0.78 - 1) = -0.11b \tag{3}$$

As shown above, three different algorithms are applied for replacement mechanisms. In Figures 4(a) to 4(e), the remaining energy for 14 drones in a swarm before and after the replacement is shown. In each replacement step, the leader drone functions as a coordinator. Once a drone with maximum energy is found, the replacement command will be issued to drones that are involved in replacement scenarios. In this replacement mechanism, just four drones are involved in the replacement process, which are leader, tail, and two drones with maximum power in the middle.

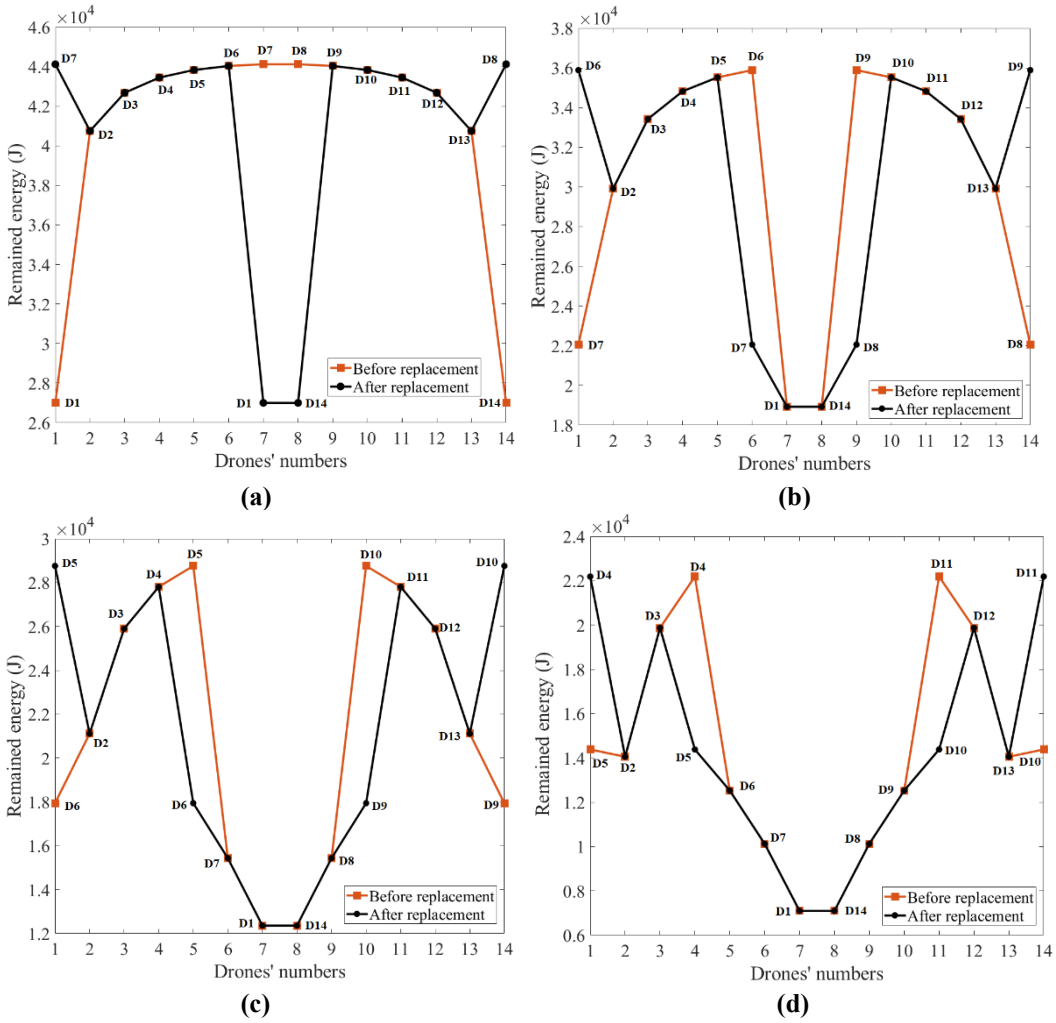

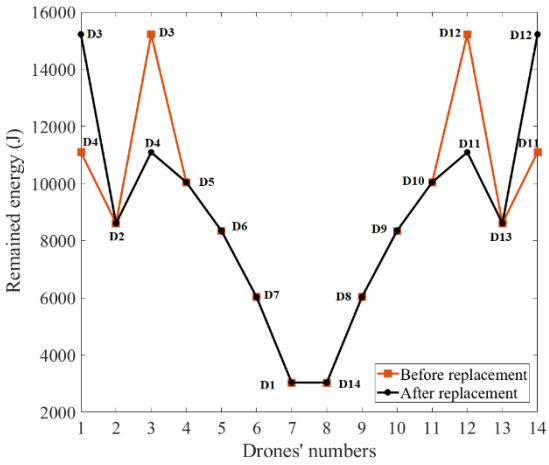

(e)

Figure 4. Remained energy of individual drones before and after replacements (leader and tail switching).

The next two replacing scenarios are two different full shuffling replacements to show that in some cases, full shuffling might be better than head and tail replacement, and in some other shuffling scenarios, it might be worse than that. The first shuffling scenario is based on replacing the drone with maximum energy with drone with the lowest energy. This method continues until all the drones are replaced with each other. Figures 5(a) to 5(e) show this shuffling scenario. Figure 5(a) demonstrates that drone one to fourteen are replaced with [D7, D6, D5, D4, D3, D2, D1, D14, D13, D12, D11, D10, D9, D8], consecutively. This shows that in each replacement step all fourteen drones are replaced with some other drones. Using this method, six different replacement steps are executed until their energy drain to one percent of their initial energy.

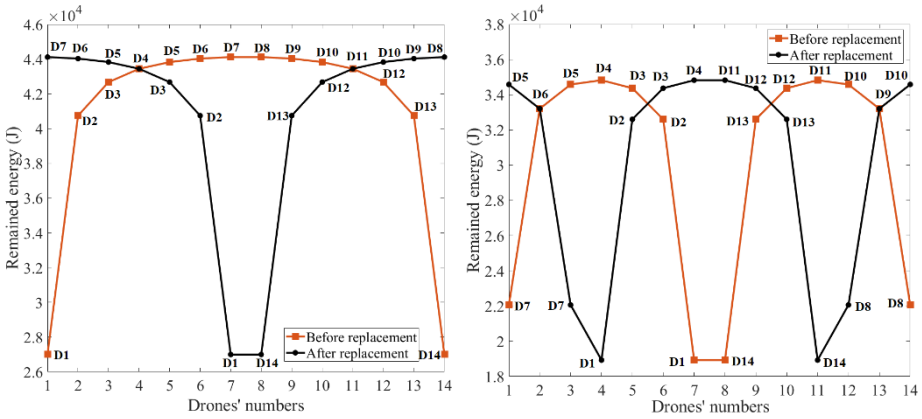

(a) **(b)**

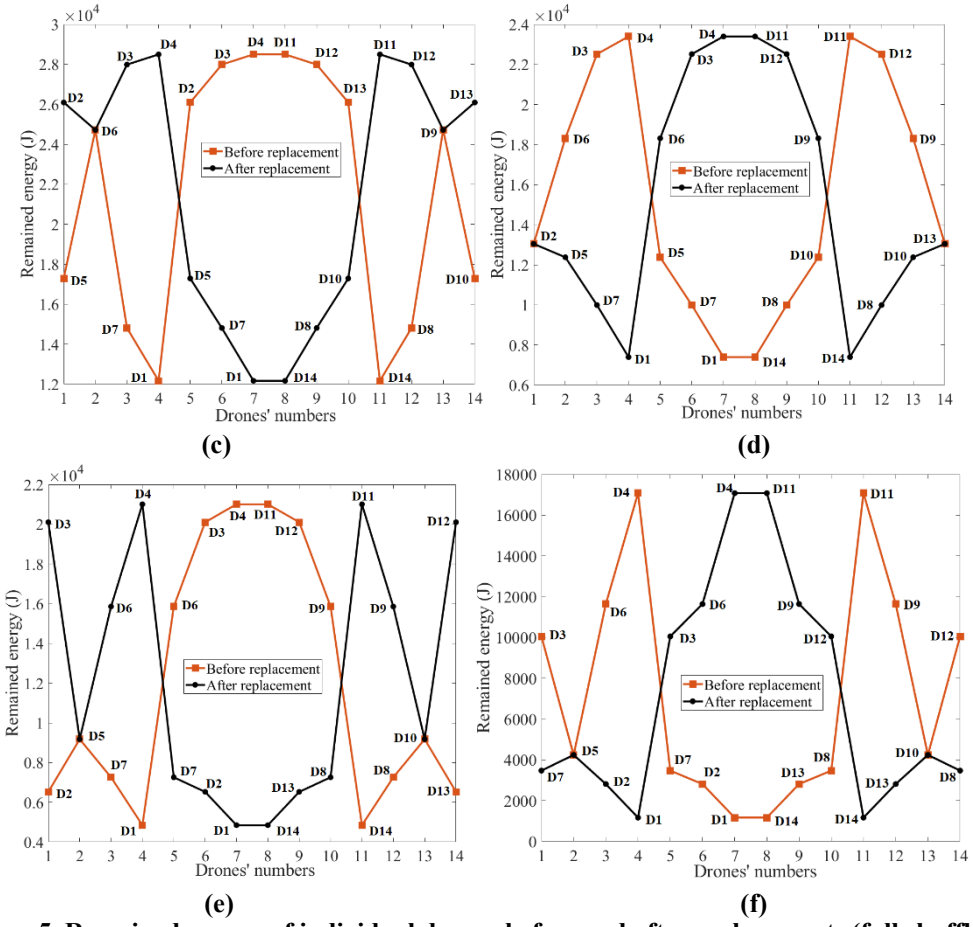

Figure 5. Remained energy of individual drones before and after replacements (full shuffle 1).

In the second shuffling method, the first two drones with maximum energy go to the lead and tail positions and the second two drones with the highest energy go to the second place behind the lead and tail drones. This process continues until all the drones are replaced in their proper positions. Figures 6(a) to 6(e) show this second shuffling replacement scenario. Figure 6(a) indicates that this method provides the same replacing order in the first step of replacement as the first shuffling method. However, starting the second step, their repositioning is different and different graphs are achieved.

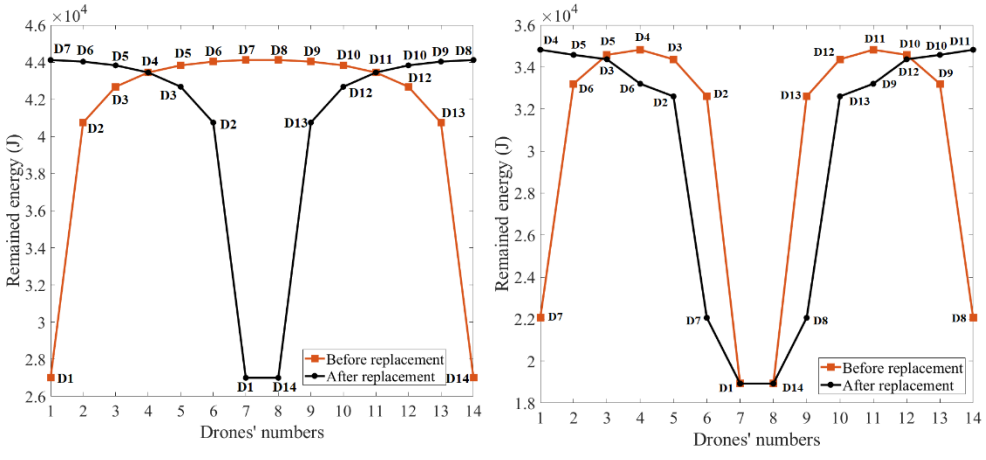

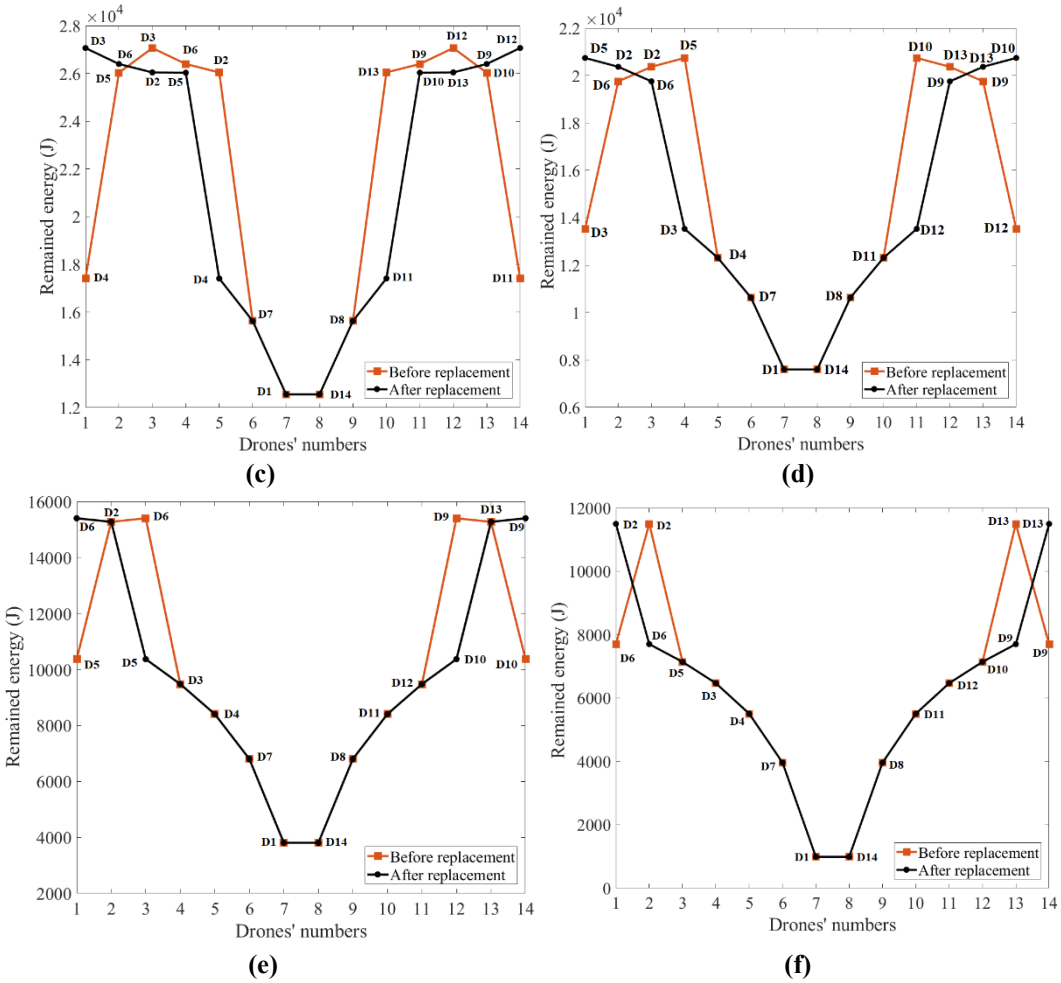

Figure 6. Remained energy of individual drones before and after replacements (full shuffle 2).

Figure 7(a) presents the different distance achieved through different replacement methods. Figure 7(b) demonstrates the cost of the above mentioned different replacement techniques. As can be seen from Figure 7(a), the swarming drones can achieve higher distances if they apply the second shuffling mechanism. This replacement mechanism (full shuffle 2) shows a 3.7% and 6.3% enhancement in achieved flight distance compared to leader and tail switching and full shuffle 1 mechanisms, respectively.

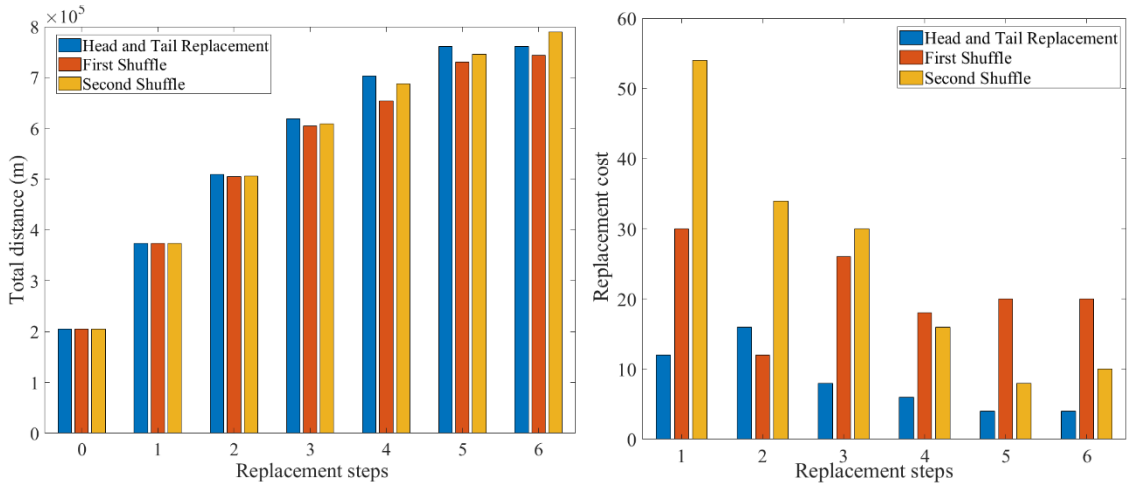

(a) **(b)**

Figure 7. View of the total (a) covered distance and (b) replacement cost for different steps.

VI. Conclusion

The sensitivity of the drag of each drone in a V-shaped swarming to the wingtip spacing and wingspan was studied. It was also shown that repositioning of the drones during the V-shaped swarming flight will enhance their efficiency and achieved distances. Two different shuffling replacement methods were compared with the head-and-tail replacement technique. In the first shuffling method, drone with the maximum energy level was replaced with drone with the minimum energy, iteratively. In the second shuffling replacement, the two drones with maximum energy replaced with the head and tail drones and the drone with the second-highest level of energy were repositioned with the two drones after the leader and before the tail drone. This repositioning was continued until all the drones were placed in their efficient positions. Our extensive analysis showed that the first shuffling is worse than the head-and-tail replacement mechanism. However, the second shuffling method showed an improvement of 3.7% and 6.3% in achieved flight distance compared to leader-and-tail switching and full shuffle 1 mechanisms, respectively.

References

[1]Hassanalian, M. and Abdelkefi, A., "Classifications, applications, and design challenges of drones: A review", Progress in Aerospace Sciences, Vol. 91, pp.99-131, 2017.

[2]Austin, R., "Unmanned aircraft systems: UAVS design, development and deployment", John Wiley & Sons, Netherland, Vol. 54, 2011.

[3]Hassanalian, M., Abdelkefi, A., Wei, M., Ziaei-Rad, S., "A novel methodology for wing sizing of bio-inspired flapping wing micro air vehicles: theory and prototype", *Acta Mechanica*, Vol. 228, No. 3, pp.1097-1113, 2017

[4]Shahmoradi, J., Mirzaeinia, A., Roghanchi, P., Hassanalian, M., "Monitoring of Inaccessible Areas in GPS-Denied Underground Mines Using a Fully Autonomous Encased Safety Inspection Drone", 2020 AIAA SciTech Forum, Orlando, Florida, 6–10 January 2020.

[5]Hassanalian, M., Salazar, R. and Abdelkefi, A., "Conceptual design and optimization of a tilt-rotor micro air vehicle", *Chinese Journal of Aeronautics*, Vol. 32, No. 2, pp.369-381, 2019.

[6]Hassanalian, M. and Abdelkefi, A., "Design, manufacturing, and flight testing of a fixed wing micro air vehicle with Zimmerman planform", Meccanica, Vol. 52, No. 6, pp.1265-1282, 2017.

[7]Sappington, R.N., Acosta, G.A., Hassanalian, M., Lee, K. and Morelli, R., "Drone Stations in Airports for Runway and Airplane Inspection Using Image Processing Techniques", In AIAA Aviation 2019 Forum, Dallas, Texas, 17-21 June 2019.

[8]Mirzaeinia, A., Hassanalian, M., Shekaramiz, M. and Mirzaeinia, M., "Loader and tester swarming drones for cellular phone network loading and field test: non-stochastic particle swarm optimization", Journal of Autonomous Intelligence, Vol. 2, No. 2, pp.14-24, 2019.

[9]Hassanalian, M., Salazar, R.D. and Abdelkefi, A., "Analysis and optimization of a tilt rotor unmanned air vehicle for long distances delivery and payload transportation. In 2018 AIAA/ASCE/AHS/ASC Structures, Structural Dynamics, and Materials Conference", Orlando, Florida, 8-12 January 2018.

[10]Mirzaeinia, A. and Hassanalian, M., "Minimum-Cost Drone–Nest Matching through the Kuhn–Munkres Algorithm in Smart Cities: Energy Management and Efficiency Enhancement", *Aerospace*, Vol. 6, No. 11, p.125, 2019.

[11]Mirzaeinia, A., Hassanalian, M., Lee, K. and Mirzaeinia, M., "Energy conservation of V-shaped swarming fixed-wing drones through position reconfiguration", *Aerospace Science and Technology*, Vol. 94, p.105398, 2019.

[12]Hassanalian, M., Pellerito, V., Sedaghat, A., Sabri, F., Borvayeh, L. and Sadeghi, S., "Aerodynamics loads variations of wings with novel heating of top surface: bioinspiration and experimental study", *Experimental Thermal and Fluid Science*, Vol. 109, p.109884, 2019.

[13]Guido, N., Mohammadi, S., Hassanalian, M. and Bakhtiyarov, S., "Surface Temperature Effects of Solar Panels of Fixed Wing Unmanned Aerial Vehicles on Flight Performance", 2019 AIAA Aviation Forum, Dallas, TX, 17-21 June 2019.

[14]Colombi, J., Jacques, D.R. and Lambach, J.L., "Integrating UAS swarming with formation drag reduction", In Systems Conference (SysCon), 2017 Annual IEEE International (pp. 1-8), 2017.

[15]Mirzaeinia, A., Bradfield, Q., Bradley, S., Hassanalian, M., "Energy Saving of Echelon Flocking Northern bald ibises with Variable wingtips spacing: Possibility of New Swarming for Drones", 2019 AIAA Propulsion and Energy Conference, Indianapolis, Indiana, 19-22 August 2019.

[16]Mirzaeinia, A., Hassanalian, M., "Energy Conservation of V-Shaped Flocking Canada Geese through Leader and Tail Switching", 2019 AIAA Propulsion and Energy Conference, Indianapolis, Indiana, 19-22 August 2019.

[17]Mirzaeinia, A., Hassanalian, M., Lee., K., Mirzaeinia, M., "Performance Enhancement and Load Balancing of Swarming Drones through Position Reconfiguration", 2019 AIAA Aviation Forum, Dallas, TX, 17-21 June 2019.

[18]Heppner, F.H., "Avian flight formations", *Bird-Banding*, Vol. 45, No. 2, pp.160-169, 1974.

[19]Badgerow, J.P. and Hainsworth, F.R., "Energy savings through formation flight? A re-examination of the vee formation", *Journal of Theoretical Biology*, Vol. 93, No. 1, pp.41-52, 1981.

[20]Hummel, D., "Aerodynamic aspects of formation flight in birds", *Journal of Theoretical Biology*, Vol. 104, No. 3, pp.321-347, 1983.

[21]Seiler, P., Pant, A., and Hedrick, K., "Analysis of Bird Formations", in Proceeding of the 41st IEEE Conference on Decision & Control, Las Vegas, Nevada, 2002.

[22]Andersson, M. and Wallander, J., "Kin selection and reciprocity in flight formation?", *Behavioral Ecology*, Vol. 15, No. 1, pp.158-162, 2004.

[23]Thien, H.P., Moelyadi, M.A. and Muhammad, H., "Effects of leaders position and shape on aerodynamic performances of V flight formation", *arXiv preprint arXiv: 0804.3879*, 2008.

[24]Nathan, A. and Barbosa, V.C., "V-like formations in flocks of artificial birds", *Artificial life*, Vol. 14, No. 2, pp.179-188, 2008.

[25]Bajec, I.L. and Heppner, F.H., "Organized flight in birds", *Animal Behaviour*, Vol. 78, No. 4, pp.777-789, 2009.

[26]Bower, G., Flanzer, T. and Kroo, I., "Formation geometries and route optimization for commercial formation flight", In 27th AIAA Applied Aerodynamics Conference, San Antonio, Texas, 22-25 June 2009.

[27]Ning, A., Flanzer, T.C. and Kroo, I.M., "Aerodynamic performance of extended formation flight", *Journal of aircraft*, Vol. 48, No. 3, pp.855-865, 2011.

[28]Pahle, J., Berger, D., Venti, M., Duggan, C., Faber, J. and Cardinal, K., "An initial flight investigation of formation flight for drag reduction on the C-17 aircraft", In AIAA atmospheric flight mechanics conference, Minneapolis, Minnesota, 13-16 August 2012.

[29]Kent, T.E. and Richards, A.G., "On optimal routing for commercial formation flight", In AIAA guidance, navigation, and control (GNC) Conference, Boston, MA, 19-22 August 2013.

[30]Kless, J.E., Aftosmis, M.J., Ning, S.A. and Nemec, M., "Inviscid analysis of extended-formation flight", *AIAA journal*, Vol. 51, No. 7, pp.1703-1715, 2013.

[31]Li, X., Tan, Y., Fu, J. and Mareels, I., "On V-shaped flight formation of bird flocks with visual communication constraints", In 2017 13th IEEE International Conference on Control & Automation (ICCA) pp. 513-518, July 2017.

[32]https://www.sensefly.com/drone/ebee-mapping-drone/, Retrieved on 30 November 2019.